*Radiat. Phys. Chem.* Vol.15, pp.9-38.
Pergamon Press Ltd. 1980. Printed in Great Britain.

# THE MEASUREMENT OF ABSORBED DOSE AND DOSE GRADIENTS

W.L. McLaughlin
Center for Radiation Research, National Bureau of Standards
Washington, D.C. 20234

## ABSTRACT

The more reliable systems and procedures of dosimetry for radiation sterilization applications are described, along with sources of uncertainty and ways to achieve optimum accuracy and reproducibility. Dosimetry practice in production must be accompanied by correct methods of dosimeter calibration to achieve measurement assurance and quality control. For routine use and for determination of dose distributions, certain thin-film dosimeters satisfying cavity-theory requirements are most suitable.

## INTRODUCTION

Dosimetry may be defined as the measurement or determination by calculation of the radiation energy deposited locally in a given material. The radiation quantity of interest is generally the absorbed dose[*].

Dosimetry has also become one of the accepted means of determining that a quantity of ionizing radiation has been great enough to achieve a specific level of sterilization [1,2][†] throughout a product with a suitable degree of certainty [3]. It is also a reasonably reliable tool for ascertaining that the radiation dose to the product has not exceeded prescribed values causing excessive latent radiation damage to the product [3].

Following these rather bold statements, however, a considerable amount of qualification is necessary. Certainly one would not depend on dosimetry data for product release without careful observance of the following precautions:

1. The specified value of minimum absorbed dose, $D_{min}$, in a given irradiated product must be based on thorough microbiological considerations, and the statistical confidence limits set on the value of $D_{min}$ as measured by dosimetry must reflect accepted statistical requirements.

2. The values of maximum acceptable dose, $D_{max}$, although generally not so rigidly set in terms of accuracy and precision limits, are based on various ultimate effects due to excess irradiation, i.e. loss in mechanical strength or flexibility, increase in coloration, evolution of gases and toxic products, etc.

---

[*] Absorbed dose, D, is the energy absorbed by an incremental volume of irradiated matter divided by the mass of that volume. A special derived unit of absorbed dose is the rad (1 rad $\equiv 10^{-2}$ J $\cdot$ kg$^{-1}$). A new SI derived unit has been named the gray (abbreviation Gy) by the Comité International des Poids et Mesuré (CIPM) (see K. Lidén, Phys. Med. Biol. 20, 1029-1030, 1975). 1 Gy $\equiv$ 1 J $\cdot$ kg$^{-1}$ = 100 rad.

[†] Sterilization being here the reduction in the populations of viable organisms by prescribed orders of magnitude.

3. Dosimetry data developed during commissioning of a sterilization process must be reassessed and determined anew with the setting of different process parameters (i.e. source activity, conveyor speed, dwell time, product arrangement and orientation, etc.) needed to achieve prescribed values of $D_{min}$ and the uniformity ratio, $D_{max}/D_{min}$, or with an appreciable change of product parameters (mean bulk density, degree of heterogeneity, dimensions, design minimum dose, etc.). Dosimetry is generally not needed to correct for routine source decay.

4. Dosimeters that are used in the product to determine dose distributions and thu to establish locations of $D_{min}$ and $D_{max}$ in a given process must have acceptable accuracy and precision at these absorbed-dose levels.

5. The traceability of dosimeter readings of dose to primary standards (e.g. absorbed dose in water) must be kept "up to date", in order to account for variation of dosimeter response with age of the dosimeter.

6. Sources of systematic error in dose interpretation must be accounted for in all applications. Examples of sources of such error are listed in Table I.

TABLE 1 Sources of Dosimetry Uncertainty

| RADIATION PARAMETERS | ENVIRONMENTAL FACTORS |
|---|---|
| SPECTRA | TEMPERATURE |
| INTENSITY | HUMIDITY |
| FRACTIONATION | ATMOSPHERE |
| DIRECTION | LIGHT |
| DOSE RANGES | IMPURITIES |

DOSIMETER PROPERTIES

MATERIAL
SIZE
SHAPE
STABILITY
AGE
BATCH
RUGGEDNESS
QUALITY CONTROL
CALIBRATION METHOD
READOUT METHOD

The aims of the present report are (1) to suggest calibration methods and dosimetry procedures needed to satisfy the ground rules listed above; (2) to suggest appropriate ways of determining absorbed dose and dose distributions in both homogeneous and heterogeneous products; (3) to account for sources of dosimetry error and imprecision.

## CALIBRATION

When using a radiation sensor to make a determination of absorbed dose at different locations in an irradiated product, the first consideration is whether or not that reading is traceable to some primary standard. In practice, traceability of dose to primary standards is generally accomplished by reference to absolute energy absorption measurements in a given material. The accepted primary instruments, calorimeters, ionization chambers, or standard chemical dosimeters, are well covered in the literature [4-8] and will not be dealt with here in detail.

Reliable dosimetry and mapping of dose gradients require large numbers of calibrate routine dosimeters, which are usually plastics, dyed plastics or certain liquid chemical solutions [8]. In some cases they may also be chemical systems giving standard radiation yields of measurable chemical species, such as cerous ions in ceric ammonium sulfate solutions. Once correct calibration procedures are established, thus assuring reliability of the chemical yields and optical absorption indices of the dosimeters, meaningful statistics can be assigned to the design of a sterilization procedure and quality control for product release.

Still another consideration is the spatial resolution desired for dose mapping throughout the product. Deep within a homogeneous product, dose readings with high spatial resolution may not be important. But in heterogenous materials or at interfaces of widely different materials or at solid surfaces, it may be necessary to use a small or thin dosimeter to get reliable readings of dose gradients. Proper calibration of such a sensor is especially important.

Suggested precautions for calibration of routine dosimeters are as follows. The radiation and environmental conditions of calibration (i.e. dose rate, spectrum, temperature, orientation, etc.) should duplicate as closely as possible the conditions of practical use [9]. Only if it is well established that the dosimeter response characteristics are the same for different irradiation conditions can calibration under conditions different from those of practical use be worthwhile. Thus, if $^{60}$Co gamma radiation or electron beams are used for production sterilization, it is best to calibrate the dosimeter response under controlled conditions in a similar field.

For calibration with $^{60}$Co gamma rays, it is important that the dosimeter be exposed between 'electron equilibrium" layers [8] of a suitable plastic material (e.g. ∿0.5 cm polystyrene). The reasons for this are: (1) dose distributions and radiation spectra are relatively free of discontinuities in the region where build-up of secondary radiations reaches a maximum; (2) the unpredictable shape of the build-up portion of the depth-dose curve can be discounted. The result is that the dose is more predictably and accurately measurable when electron equilibrium conditions are met than when a bare dosimeter is situated at the surface or near the interface of widely different media. Sources of error in calibration, such as variations in incident spectra and anomalies in radiation field and absorber geometry, are thus minimized. Once the response characteristics of the dosimeter are established by careful calibration it can be used under extreme geometric conditions, including locations at surfaces and near interfaces to give dose interpretations in a thin medium. The degree to which spatial variations of dose can be resolved, of course, will depend on the dimensions of the calibrated dosimeter.

As mentioned earlier, calibration of dosimeters for use in electron beams can be accomplished with known $^{60}$Co gamma radiation fields only if the dosimeter is known to have a response free of rate dependence, energy dependence, temperature dependence, etc. Otherwise, the calibration should be performed using a calorimeter having a geometry and constituents similar in terms of density and electron collision stopping power to those of the dosimeter in question. If this is not possible, both calorimeter and dosimeter being calibrated must have absorption characteristics well documented over a given electron spectrum. Moreover, the spectrum itself should be known approximately.

For the most common source of ionizing photons used in radiation sterilization ($^{60}$Co), the degraded spectrum falls mainly between about 0.05 and 1.33 MeV in energy. With the upper part of the spectrum, corrections for departures from ideal cavity theory conditions are minor [10], so that fairly simple ratios of energy absorption coefficients and electron stopping powers can generally be used to calculate dose in one material based on experimental determinations of dose in another material [8, 11,12]. Fig. 1 shows examples of degraded spectra calculated for different depths in a water absorber irradiated by a semi-infinite $^{60}$Co plaque source [13]. Similar spectra occur inside the cylindrical chamber of the $^{60}$Co gamma-ray calibration source at NBS (presently ∿12 kCi) [14-16] and inside a typical AECL Gammacell 220 used for calibration of dosimeters [17].

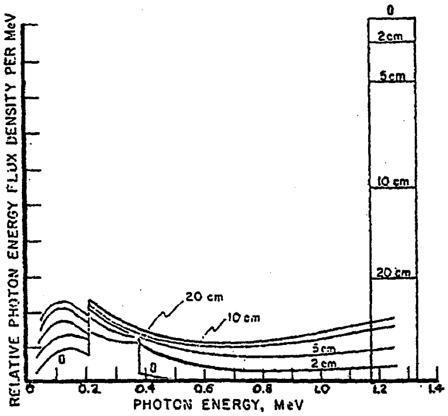

Fig. 1. Calculated photon spectra including single and multiple scattering at various depths in a semi-infinite slab of water irradiated from one side by a large $^{60}$Co plaque source [13]. The spectra are given in terms of relative photon energy flux density per MeV interval as a function of photon energy in MeV. The areas under the vertical bars represent relative amounts of primary energy (average 1.25 MeV) remaining at each depth (in cm). The degraded photon spectra at these depths are given by the curves from 0.04 to 1.25 MeV. The relative areas under these curves represent photon energy occurring as scattered radiation.

If a dosimeter being calibrated is sufficiently small relative to the range of secondary electrons (i.e. sufficiently non-disruptive to the radiation field to comply with cavity theory requirements [10,18,19]) and is placed inside another material thick enough to provide approximate electron equilibrium conditions, most of the dose to the small dosimeter is due to secondary electrons produced in the surrounding material. In this case, the absorbed dose in the enclosed dosimeter material is related to absorbed dose in the surrounding material by ratios of respective electron collision stopping powers [20,21] averaged over the approximate electron spectrum at the site of irradiation (See Table II).

One must also consider the problem of relating dose in one surrounding material, that is, in the relatively thick layer required for electron equilibrium, to dose in the material used for calibration, that is, primary dosimeter material that was used to establish the dose rate in the gamma radiation field. To accomplish this, it is necessary to multiply by the ratios of mass energy absorption coefficients ($\mu_{en}/\rho$) averaged over the approximate photon spectrum at the location of irradiation [22]. Table III lists ratios, water-to-material, of $\frac{\mu_{en}}{\rho}$ for different materials, for the mean primary $^{60}$Co gamma-ray energy (1.25 MeV) and for typic degraded $^{60}$Co gamma-ray spectra.

## DOSIMETER MATERIALS

Typical used primary standard dosimeters are as follows:

1. Calorimeters [4,5]: pure graphite (carbon); aluminum; water; "muscle-equivalent" conducting plastic (polyethylene containing certain fillers) [23]

2. Ionization chambers [7]: Air-filled chamber made of graphite or "muscle-equivalent" conducting plastic [23]

3. Chemical dosimeters [5,24]: Ferrous sulfate ("Fricke) solution [8,12,24,25]; ceric sulfate solution [12,24,26,27]

Typical secondary dosimeter materials used with spectrophotometric or, in some cases, potentiometric analysis for routine applications are as follows:

| | |
|---|---|
| 1. Liquid solutions: | ethanol-chlorobenzene [5,28-30]<br>ceric-sulfate plus cerous-sulfate [31]<br>radiochromic dyes [8,12,32,33] |
| 2. Undyed plastics: | polymethyl methacrylate ("clear Perspex") [34]<br>cellulose triacetate [35]<br>polyethylene [36,37] |
| 3. Dyed plastics: | polymethyl methacrylate (red or amber Perspex)[38]<br>Nylon or polyvinyl butyral [8,12,39,40]<br>Cellophane or Cinemoid [41,42] |

The latter groups of dosimeters need calibration in a known radiation field before they can be used successfully.

Other promising routine dosimeters are d-alanine, which is analyzed by electron spin resonance spectroscopy [43,44] and glutamine, which undergoes lyoluminescence when dissolved after irradiation [45,46].

TABLE II Ratio of Mass Collision Stopping Power for Electrons in Water Relative to That in Different Substances and Dosimeter Materials

$$\left[\frac{1}{\rho}\frac{dE}{dx}\right]_{water} \Big/ \left[\frac{1}{\rho}\frac{dE}{dx}\right]_{material}$$

| Electron Energy (MeV) | Muscle | Compact Bone | Fricke Dosimeter | Polystyrene $(C_8H_8)_n$ | Perspex $(C_5H_8O_2)_n$ | Polyethylene $(C_2H_4)_n$ | LiF | Glass[a] | PVC |
|---|---|---|---|---|---|---|---|---|---|
| 0.05 | 1.02 | 1.09 | 1.01 | 1.03 | 1.03 | 0.948 | 1.26 | 1.26 | 1.26 |
| 0.1 | 1.01 | 1.09 | 1.01 | 1.03 | 1.03 | 0.951 | 1.25 | 1.24 | 1.23 |
| 0.15 | 1.02 | 1.08 | 1.01 | 1.03 | 1.03 | 0.952 | 1.25 | 1.24 | 1.22 |
| 0.2 | 1.02 | 1.08 | 1.01 | 1.03 | 1.03 | 0.953 | 1.25 | 1.24 | 1.22 |
| 0.3 | 1.02 | 1.08 | 1.01 | 1.03 | 1.03 | 0.956 | 1.25 | 1.23 | 1.21 |
| 0.4 | 1.02 | 1.08 | 1.00 | 1.03 | 1.04 | 0.960 | 1.25 | 1.23 | 1.21 |
| 0.5 | 1.03 | 1.08 | 1.00 | 1.04 | 1.04 | 0.963 | 1.25 | 1.23 | 1.21 |
| 0.6 | 1.03 | 1.08 | 1.00 | 1.04 | 1.04 | 0.965 | 1.25 | 1.23 | 1.21 |
| 0.7 | 1.03 | 1.08 | 1.00 | 1.04 | 1.04 | 0.967 | 1.25 | 1.22 | 1.21 |
| 0.8 | 1.02 | 1.08 | 1.00 | 1.04 | 1.05 | 0.969 | 1.25 | 1.22 | 1.20 |
| 0.9 | 1.03 | 1.08 | 1.00 | 1.04 | 1.05 | 0.970 | 1.25 | 1.22 | 1.20 |
| 1.0 | 1.03 | 1.08 | 1.00 | 1.04 | 1.05 | 0.971 | 1.25 | 1.21 | 1.20 |
| 2.0 | 1.03 | 1.08 | 1.00 | 1.05 | 1.05 | 0.977 | 1.25 | 1.19 | 1.17 |
| 3.0 | 1.02 | 1.08 | 1.00 | 1.05 | 1.06 | 0.981 | 1.25 | 1.18 | 1.15 |
| 4.0 | 1.02 | 1.08 | 1.00 | 1.05 | 1.06 | 0.982 | 1.26 | 1.17 | 1.13 |
| 5.0 | 1.02 | 1.08 | 1.00 | 1.05 | 1.06 | 0.983 | 1.26 | 1.16 | [illegible] |
| 6.0 | 1.02 | 1.08 | 1.00 | 1.05 | 1.06 | 0.984 | 1.26 | 1.15 | 1.13 |
| 7.0 | 1.02 | 1.08 | 1.00 | 1.05 | 1.06 | 0.985 | 1.27 | 1.15 | 1.13 |
| 8.0 | 1.02 | 1.08 | 1.00 | 1.05 | 1.06 | 0.986 | 1.27 | 1.14 | 1.13 |
| 9.0 | 1.02 | 1.08 | 1.00 | 1.05 | 1.06 | 0.987 | 1.27 | 1.14 | 1.13 |
| 10.0 | 1.02 | 1.08 | 1.00 | 1.06 | 1.06 | 0.988 | 1.27 | 1.14 | 1.12 |

[a] Typical Pyrex glass: 80.7% $Si_2O$, 12.9% $B_2O_3$, 3.8% $Na_2O$, 2.2% $Al_2O_3$, 0.4% $K_2O$

Other materials have also been shown to be useful for the routine determination of large radiation doses, but the ones most widely used are among those listed above. Physical properties and useful dose ranges of these systems are compiled in the literature [4,5,8,9,11,12,24].

The most important dosimeters for routine use are those that are commercially available in large batches and that are capable of relatively reproducible dose interpretations by means of spectrophotometric readings of optical density at given wavelengths. Typical absorption spectra and response curves for some of the commercially available routine dosimeters are given in Figs. 2, 3, and 4.

TABLE III Ratio of Photon Mass Energy Absorption Coefficients of Water to Those of Different Absorbing Materials, for Primary and Typical Degraded $^{60}$Co γ-ray Spectra [22]

| | $(\mu/\rho)^{en}_{water} / (\mu/\rho)^{en}_{material}$ | | |
|---|---|---|---|
| Material | Primary (1.17 MeV, 1.33 MeV) | Degraded Spectrum in Gammacell 220[a] [17] | Degraded Spectrum at 10 cm Depth in Semi-infinite Water from Large Plaque Source [13] |
| Muscle | 1.01 | 1.01 | 1.01 |
| Compact bone | 1.05 | 1.03 | 1.04 |
| Fricke dosimeter (ferrous sulfate sol.) | 1.00 | 1.00 | 1.00 |
| 0.015 M ceric ammonium sulfate sol.) | 1.01 | 0.97 | 0.98 |
| Polystyrene | 1.03 | 1.06 | 1.07 |
| Polymethyl methacrylate | 1.03 | 1.04 | 1.06 |
| Nylon | 1.01 | 1.03 | 1.04 |
| Polyethylene | 0.97 | 0.98 | 0.98 |
| LiF | 1.20 | 1.18 | 1.18 |
| Glass[b] | 1.11 | 0.96 | 0.98 |
| Polyvinyl chloride | 1.11 | 0.80 | 0.82 |
| Carbon | 1.11 | 1.11 | 1.12 |
| Aluminum | 1.15 | 0.69 | 0.71 |
| Iron | 1.18 | 0.28 | 0.30 |

---

[a] This spectrum is approximated from spectral measurements with a cylindrical NaI crystal, with the results weighted for energy dependence of the response of NaI to ionizing photons. Geometry factors and self-attenuation by the detector are not taken into account.

[b] Typical Pyrex Glass [22]: 80.7% $Si_2O$, 12.9% $B_2O_3$; 3.8% $Na_2O$, 2.2% $Al_2O_3$, 0.4% $K_2O$.

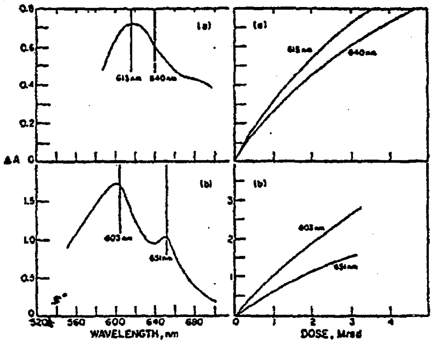

Fig. 2. For two dyed polymethyl methacrylate dosimeters of 3 mm thickness: (a) red Perspex type 4034; (b) amber Perspex type 3042, change in optical density (ΔA) versus wavelength is shown at the left, and change in optical density versus absorbed dose in polymethyl methacrylate is shown at the right [11]. The vertical lines on the left-hand plots indicate typical wavelengths for spectrophotometric analysis. The curves on the right were made at those indicated wavelengths.

## ROUTINE DOSIMETRY PROBLEMS

In selecting a practical dosimetry system, or better, systems, since it may be best to to have a calibrated back-up system available, one must decide on such factors as dose range, need for stability, probable environmental conditions (e.g. temperature during and after irradiation), batch size, availability, precision and accuracy limits needed, readout methods available, and special requirements of the dosimeter

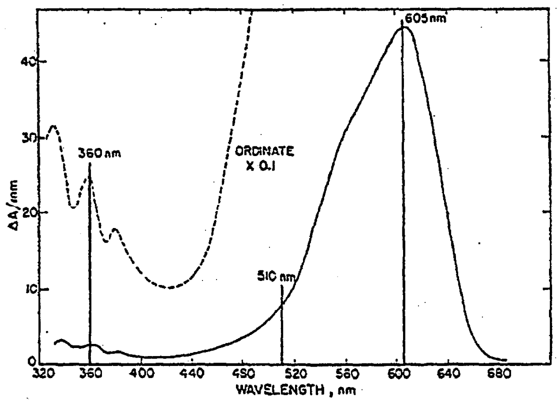

Fig. 3. For nylon radiochromic dosimeter film (Far West Technology type 60) the absorption spectrum due to irradiation to an absorbed dose of 2.5 Mrad (25 kGy), in terms of change in optical density per unit thickness (ΔA/mm) as a function of analyzing wavelength, is shown [15]. The vertical lines indicate typical wavelengths for analysis during calibration.

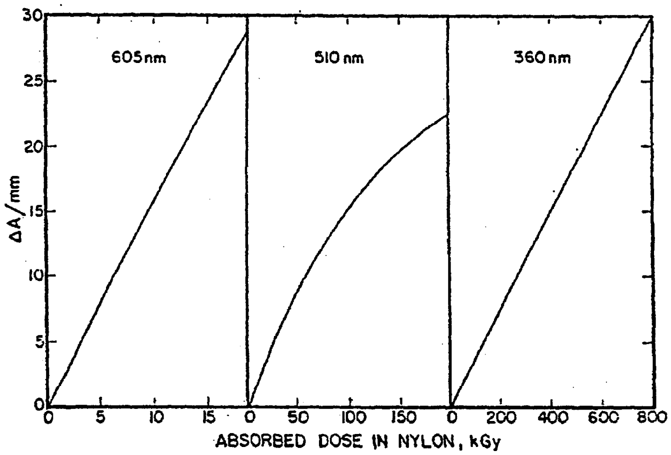

Fig. 4. For the same dosimeter at that in Fig. 3, the change in optical density per unit thickness at the indicated wavelengths is shown as a function of absorbed dose in nylon [15].

(e.g., dose field mapping, measurement of transit dose, radiobiological studies in the range 0.1 - 1.0 Mrad, interface or surface dose determinations). One must also have knowledge of rate and energy dependence factors. Most important of all, one must have available a reliable means of calibration and have traceability to a primary standard absorbed-dose calibration in a given material (e.g. water) within prescribed limits of uncertainty.

Some sources of uncertainty in dose interpretations will now be discussed and examples will be given on how to make suitable corrections where possible, in order to minimize the uncertainties.

## 1. Calibration

Since most routine dosimeters have radiation response characteristics that change from batch to batch or with time, calibration must be kept up to date, or at least an in-house method of monitoring such changes must be available. Calibrations can be kept traceable to National Laboratories, either directly or through regional or industrial calibration labs or by round-robin intercomparisons [4,15]. If the production facility performs its own periodic calibration checks after establishing traceability of its routine dosimeter reading to a primary standard, there must also be confidence that all sources of systematic error are considered and that the in-house calibration procedure follows good dosimetry methods. Examples of pitfalls in this practice are:

a. Ignoring the effect of energy dependence due to differences in spectral degradation.

b. Poor control of geometric factors, either in reproducing dosimeter position or in control of surrounding scattering material.

c. Not accounting for differences in environmental conditions (light, humidity, temperature, etc.) that might affect dosimeter response.

d. Not accounting for anomalies caused by aging of the dosimeter or instabilities (e.g. fading) between irradiation and readout.

e. Ignoring possible changes in performance of the readout equipment itself.

f. Poor handling of the dosimeters and readout instruments (operator errors).

g. Not keeping up with batch-to-batch changes of response and departures from linearity of response curve shape at deviated dose levels.

h. Attempting to use the dosimeter outside of its accepted useful range of dose or dose rate.

## 2. Energy Dependence

We have already seen that photon absorption cross-sections and electron stopping powers are not the same for different materials and, moreover, vary appreciably with energy over the range 0.05 to 1.5 MeV, particularly in the lower part of this energy region (see Tables II and III). It has been shown that photon and electron spectra vary with depth of penetration, mainly because of multiple-scattering degradation of secondary radiations [8,13]. Because of these effects, the response of a given dosimeter, even if it is a plastic material, differs from that to water or a biological system, especially if there is an appreciable fraction of low-energy radiations (<0.2 MeV) at the site of irradiation.

Fig. 5 shows examples of calculations of energy dependence of dosimeter response relative to absorption by biological tissue (muscle), the variations being due to different additives in a radiochromic dosimeter material. The curves are ratios of energy absorption coefficients, dosimeter-to-muscle, as functions of photon energy. The response differences averaged over this energy region for broad graded $^{60}$Co gamma-ray spectra will be much less severe, but, because there is an preciable fraction of low-energy photons and electrons within an irradiated oduct, energy dependence of response can be a problem. This is especially true the hydrogen content of the product or dosimeter material is widely varying, if there is a marked difference in content of higher atomic number materials, ch as glass, metals, halogens, etc.

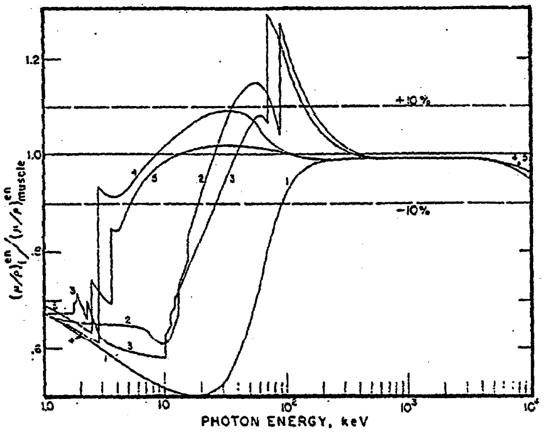

Fig. 5. For a plastic radiochromic dye dosimeter, ratios of total mass energy absorption coefficients, dosimeter (i)-to-muscle, as a function of photon energy:

1. "standard" dosimeter (no additive)
2. additive 0.6% Pb acetate
3. additive 0.4% phosphotungstic acid
4. additive 8.2% polyvinyl chloride
5. additive 5% potassium pyrosulfate

As an example, even with a relatively low concentration of ceric ammonium sulfate (0.015 molar) in water containing 0.4M $H_2SO_4$, the effect of energy dependence is calculated to be appreciable for typically degraded $^{60}$Co gamma-ray spectra (see Table III). Although some experimental evidence appears to contradict this effect [48], calculations predict a measurable energy dependence of response even for the low concentrations of ferrous sulfate (1 mM) in the ferrous sulfate dosimeter [49], if there is an appreciable component of low energy radiations.

The spectral energy ranges in most radiation sterilization applications are generally not extreme enough to cause variations in response due to differences in linear energy transfer. The physical or chemical dosimeter, however, may have a fundamental response function greatly different from a biological system, whose survival curve shapes are usually tempered by recovery effects at low doses, especially with the low relative biological effectiveness of minimum specific-ionization radiations.

### 3. Dose-Rate Dependence

There are two main forms of dependence of response due to absorbed-dose rate differences. At very low dose rates, reverse reactions and other fading effects in unstable systems may cause an unexpected lowering of sensitivity relative to that at higher dose rates. At very high dose rates, competing interaction mechanisms may cause excess energy that is deposited in a relatively short time to be unmeasurable. Short-term saturation or fatigue effects are common causes for high-intensity rate dependence in many chemical radiation sensors [50].

Fractionation of the total dose, that is, a series of interrupted irradiations, such as occurs with indexing of the product in multiple conveyor passes by a source plaque, or with electron beam scanning, can cause a reduction in effective response relative to that of a continuous irradiation used in calibration [9,11].

### 4. Temperature Dependence

A typical temperature rise during a product irradiation in a very large $^{60}$Co gamma ray facility is shown in Fig. 6 [51]. For such an extreme situation, thermal effects during and after irradiation are a common source of error in making dose interpretations. An example of the effects of variations of temperature during irradiation is shown in Fig. 7 for radiochromic dye film response [52]. Because of this effect, it is necessary to know approximately the average temperature during product irradiation so that corrections can be applied to the dose interpretation, since calibration is generally made at a lower temperature. The effect of post irradiation temperature variations on radiochromic dosimeter response is negligible [52].

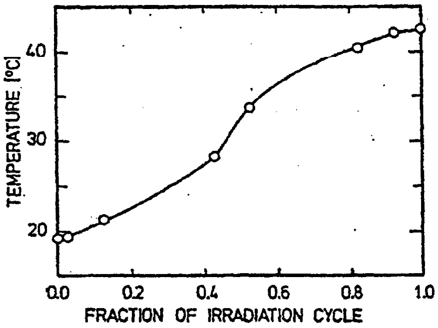

Fig. 6. Typical variation in temperature in an irradiated box containing medical products during sterilization as it is goes on a conveyor past a very large $^{60}$Co plaque along with other product boxes, as a function of fractions of the total irradiation cycle [51].

Figure 8 shows that red Perspex type 4034 has a less marked temperature dependence of response at least at temperatures less than 60°C. The fact that the temperature dependence curve shapes differ at different dose levels is more clearly understood in terms of spectral absorption curves for different temperatures during irradiation (see Fig. 9) [51]. Although the dosimeter batches differ in these two figures (batches D and B, respectively), the trend is the same for both batches.

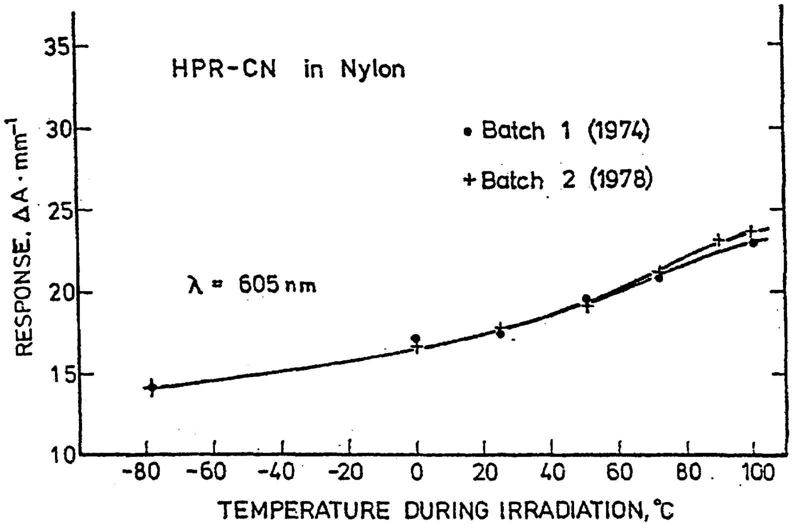

Fig. 7. Variation of response of two commercial batches of nylon radiochromic dye film, measured at 605 nm wavelengths, as a function of temperature during irradiation [52]. Absorbed dose = 1.5 Mrad.

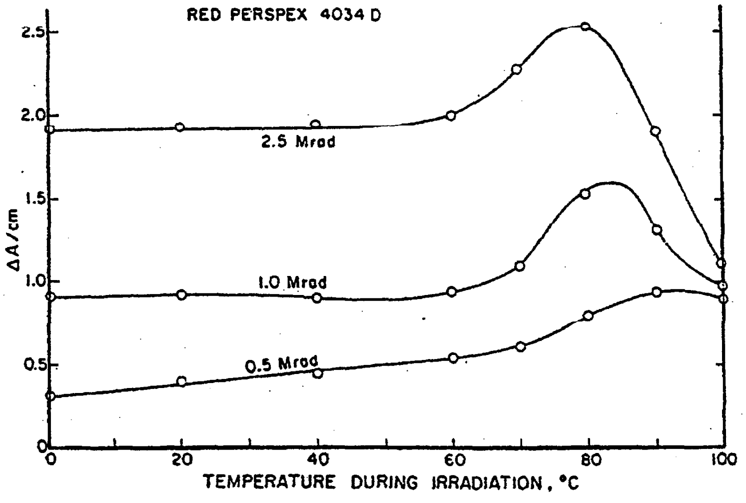

Fig. 8. Variation of response of red Perspex, type 4034, batch D, measured at 640 nm wavelengths as a function of temperature during irradiation, for the three indicated values of absorbed dose [52].

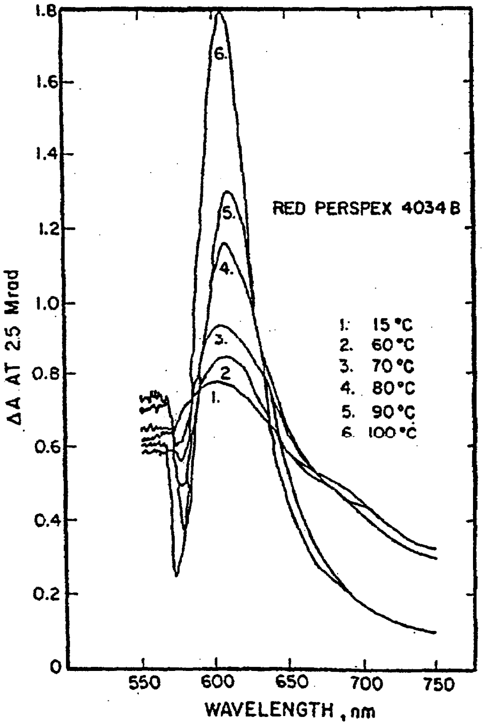

Fig. 9. For red Perspex dosimeter type 4034, batch B, absorption spectra in terms of change in optical (ΔA) due to irradiation at various temperatures to 2.5 Mrad dose, as a function of wavelength of analysis [51].

Perhaps a more serious problem with the red Perspex dosimeter is the effect of extreme temperatures during the storage period after irradiation [53]. For example, during a relatively long period of several hours when the dosimeter remains in a product that retains heat built up during irradiation, the dosimeter instability factors (see below) differ from those due to normal room-temperature storage encountered by calibration films. This effect may cause appreciable errors in dose interpretation unless suitable correction factors are applied.

## 5. Instabilities

There are two major forms of instabilities affecting routine dosimeter response. One is the variation of dosimeter response characteristics with age of the dosimeter.

The other is the (latent) fading or growth of optical density (or other signal) between irradiation and read-out. Fig. 10 shows changes of radiation-induced optical absorption in nylon radiochromic dye film at strategic wavelengths of analysis, as a function of storage time under normal room temperatures between irradiation and readout [52]. Figs. 11 and 12 show similar curves for two batches of

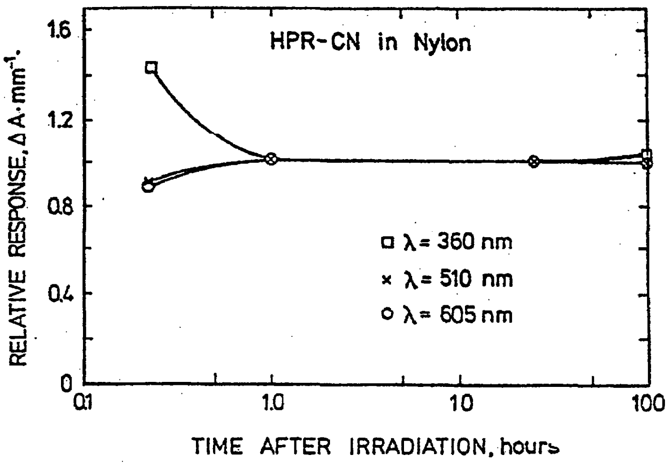

Fig. 10. Variations in relative values of $\Delta A \cdot mm^{-1}$ of nylon radiochromic dye film dosimeter, for different storage times after 2-MeV electron irradiation to 2.5 Mrad, using three optical wavelengths of analysis [52].

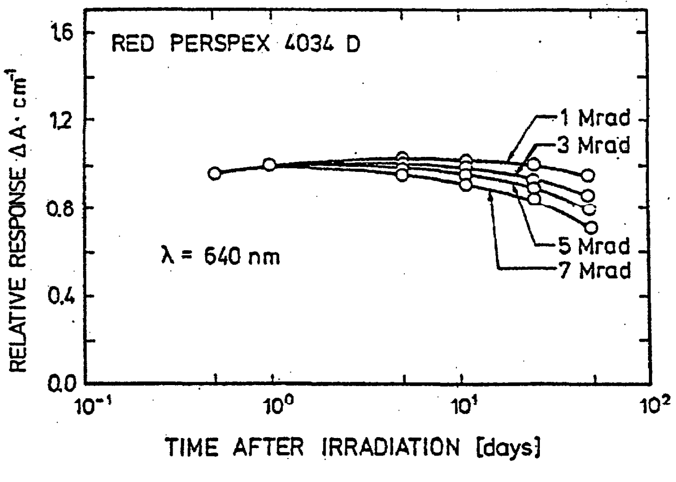

Fig. 11. Variations in relative values of $\Delta A \cdot mm^{-1}$ of red Perspex dosimeter type 4034, batch F, for different storage times after 2-MeV electron irradiation to different doses, using the indicated optical wavelength of analysis [52].

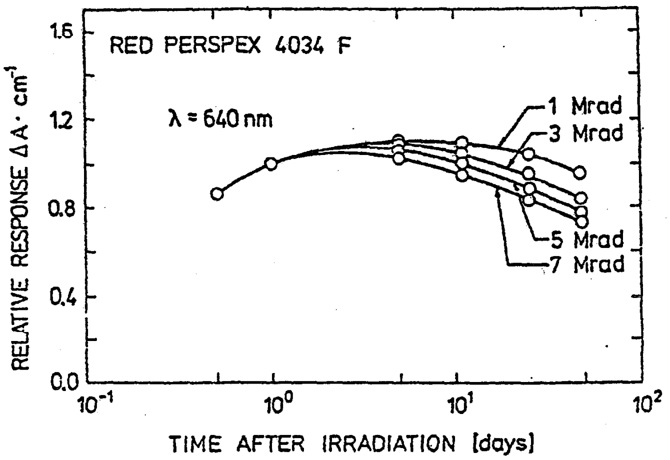

Fig. 12. Variations in relative values of ΔA · mm$^{-1}$ of red Perspex dosimeter type 4034, batch F, for different storage times after 2-MeV electron irradiation to different doses, using the indicated optical wavelength of analysis [52]

red Perspex type 4034, and different dose levels. Figs. 13 and 14 show the red Perspex fading data in terms of response curve shape changes, which are more severe

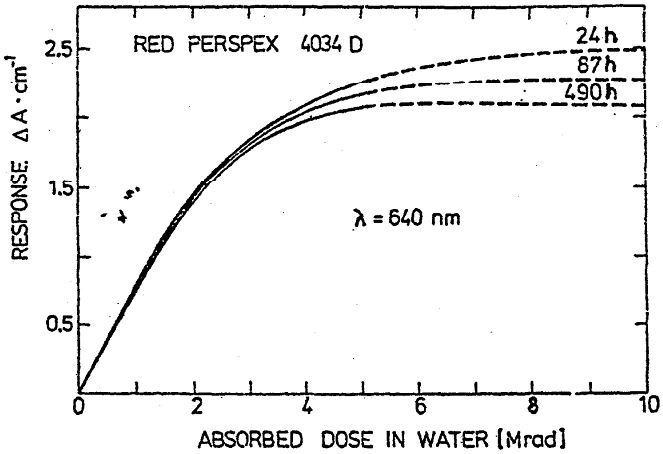

Fig. 13. Response curves (ΔA · cm$^{-1}$ dose in water) for red Perspex dosimeter type 4034, batch D, when analyzed at the indicated wavelength at different times after irradiation with $^{60}$Co gamma radiation [52].

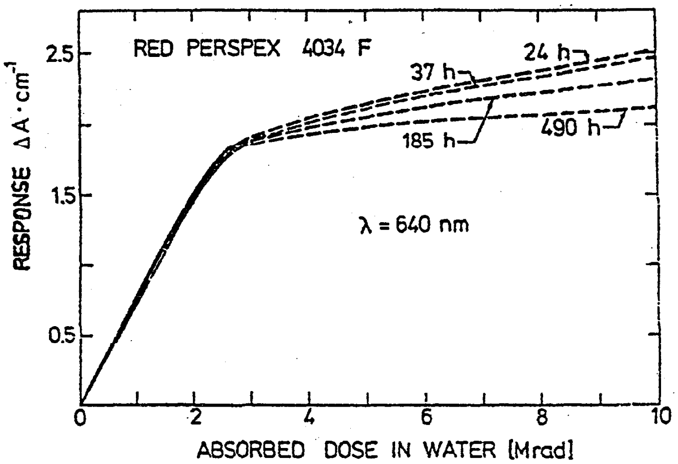

Fig. 14. Response curves ($\Delta A \cdot cm^{-1}$ versus dose in water) for red Perspex dosimeter type 4034, batch F, when analyzed at the indicated wavelength at different times after irradiation with $^{60}Co$ gamma radiation [52].

at the higher dose levels (It is interesting to observe differences in temperature dependence and response curve shapes between the two batches.) Other forms of dyed Perspex may show still different anomalies in response characteristics.

## 6. Humidity Dependence

The effect of moisture and changes of relative humidity (r.h.) is difficult to determine precisely, because of the long conditioning times required for thicker plastic dosimeters. Even if the conditioning period is relatively short (approximately 10 hours) before irradiation at extreme values of r.h., thin dosimeters such as nylon radiochromic dye films show marked reduction in response (see Fig. 15) [46]. On the other hand, for the thin films (50 µm thickness) irradiated at approximately 50 percent r.h., but stored for different times at various values of r.h., there is very little effect on response. Fig. 16 shows that for a 16-h preconditioning of the thicker red Perspex dosimeter (∿3.0 mm thickness), there is a relative humidity effect on response during irradiation only at the highest relative humidity used in the study (97% r.h.). Much longer preconditioning in the absence or presence of moisture, however, shows more pronounced response differences [53].

## 6. Dosimeter Size and Shape

A frequently neglected concept in practical dosimetry is the dosimeter size, as well as its orientation relative to the main direction of the penetrating radiation in an extended medium [54]. A fairly dense and bulky dosimeter placed in a medium of relatively low bulk density may disturb the continuity of the radiation field and its energy deposition profile, thus causing an unrealistic dose reading. This is particularly the case when the quantity of interest is absorbed dose in biological materials, water, or low atomic number plastics, and the dosimeter contains relatively high atomic number substances, such as glass, halogens, or conventional thermoluminescence materials. This effect was discussed earlier in the section on energy dependence.

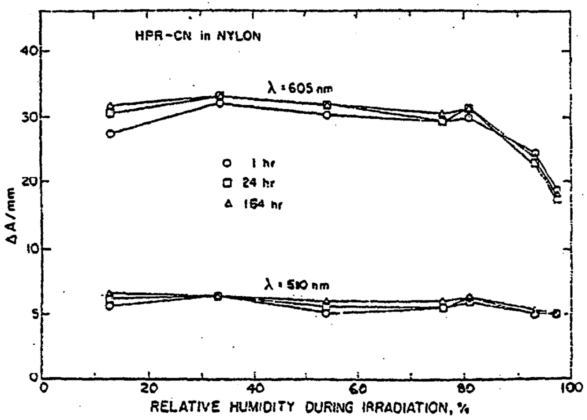

Fig. 16. Variation of response of nylon radiochromic dye film dosimeter measured at two wavelengths, as a function of relative humidity during irradiation, for the different indicated storage periods at 54% relative humidity. Absorbed dose = 2 Mrad.

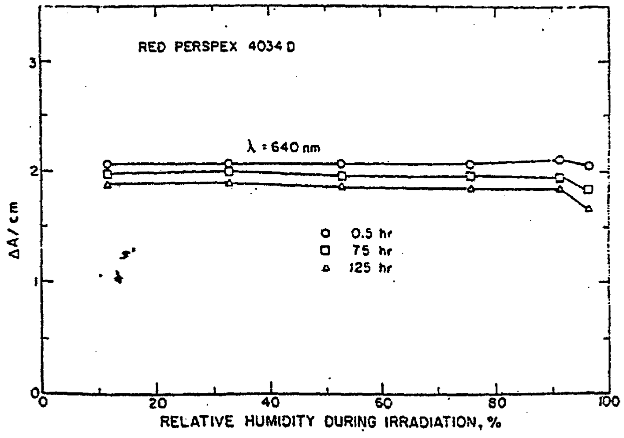

Fig. 16. Variation of response of red Perspex dosimeter type 4034, batch D, measured at 640 nm wavelength, as a function of relative humidity during irradiation for the different indicated storage periods at 54% relative humidity [52]. Absorbed dose = 3 Mrad.

Directional dependence of response is especially important for plane-parallel incidence of relatively low-energy radiations on bare thin dosimeters. It is clear that suitable precautions are necessary when using thin dosimeters at exterior surfaces of irradiated products or completely bare in an irradiation field. The thin sensor that has been calibrated under conditions approximating electron equilibrium will then simply measure according to its situation, that is, the dose in a thin layer on a surface or in a thin unmoderated layer in air. In addition, a thin-layer sensor, or a stack of thin dosimeters, placed at various locations on the surface or inside a medium of relatively low bulk density, gives a more realistic dose interpretation than does a thick dosimeter, because of cavity-theory considerations [10, 18,19].

Fig. 17 shows that even for such penetrating photons as $^{60}$Co gamma radiation, the size and shape of calibrated dosimeters relative to orientation of the irradiation (plane-parallel or cylindrically isotropic) affect relative dose interpretations appreciably [12]. In this figure, the polystyrene wall thicknesses are all 0.475 cm,the cylindrical inner diameter is 1.2 cm, and the thin-film compartment depth is 0.1 cm in depth.

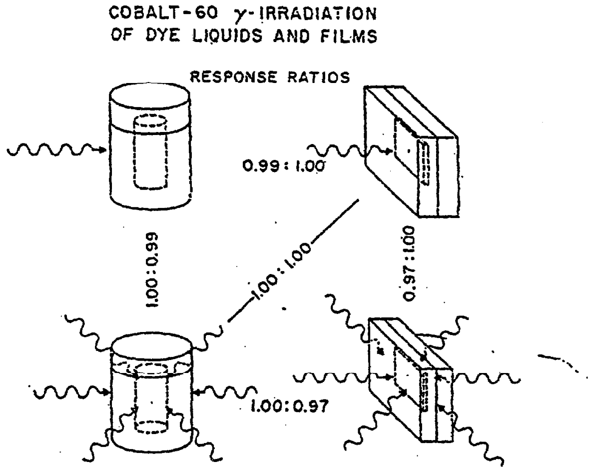

Fig. 17. Ratios of dose interpretations of different irradiation geometries for dosimeters held in plastic shells having a thickness approximately sufficient to supply electronic equilibrium (0.47 cm) and irradiated with $^{60}$Co gamma rays. Left: Cylindrical dosimeters; Right: thin film dosimeters; Top: Monodirectional parallel beam; Bottom: Isotropic radiation field [16].

Another example of the effect of dosimeter volume on $^{60}$Co gamma-ray response is shown in Fig. 18 [55]. The relative responses of two sizes of spherical graphite-wall air ionization chambers are shown as a function of the wall thickness. The dashed lines are extrapolations to zero wall thickness, whereas measurements for thinner walls would curve downward as the wall thickness dimimishes. Moreover, the shape of this "buildup curve" near zero wall thickness would vary greatly with the degree of diffuseness and energy degradation of the incident gamma ray beam.

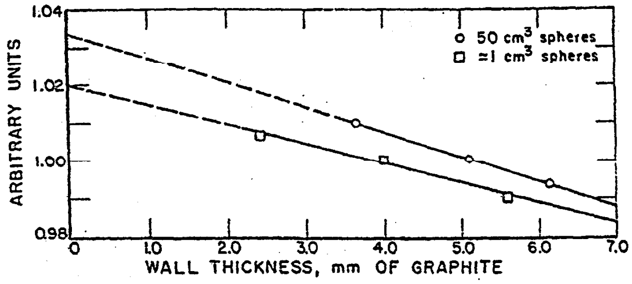

Fig. 18. Variation in relative ionization current reading given in arbitrary units as a function of thickness of graphite walls of spherical air cavity ionization chambers, for the two indicated spherical cavity volumes [55].

An advantage of using thin dosimeters is illustrated in Fig. 19, where measured absorbed dose in units of kilograys is plotted as a function of distance from the inner wall of a 2 ml cylindrical glass ampoule used to hold a liquid chemical dosimeter [16]. The measurements were made with very thin polyvinyl pyrrolidone radiochromic dye films stacked in 17 layers close to the inner glass wall. There was also a stack of these films at the center with low-density polyethylene cylinders ($\rho$ = 1.04 g/cm$^3$) filling the remainder of the glass ampoule during irradiatio by cylindrically isotropic $^{60}$Co gamma rays. The glass ampoule wall thickness is 0.6 mm, and its inner diameter is 1.06 cm. As shown by the readings of the dosimeter films close to the glass wall, the dose distribution increases in the region where there is a relatively large concentration of low-energy secondary electrons originating in the higher electron-density medium.

The effect of the electron scatter from a denser higher atomic-number medium is also illustrated in Fig. 20. The curve is a microdensitometer scan of a film strip that was placed nearly perpendicular to an interface of aluminum and nylon during irradiation from the left by a plane-parallel beam of $^{137}$Cs gamma radiatio

## 8. Placement of Dosimeters for Dose Mapping

One of the most important uses of routine dosimeters is the determination of absorbed dose profiles within irradiated products. In many applications where the product is relatively uniform and homogeneous (see Figs. 21 and 22), this is a fairly simple operation [56]. In these cases, a gamma-ray irradiation by a plaqu source symmetrically from both sides of the product (S and N) gives a somewhat symmetric dose distribution, as shown in Fig. 23 [57], where the minimum dose lie

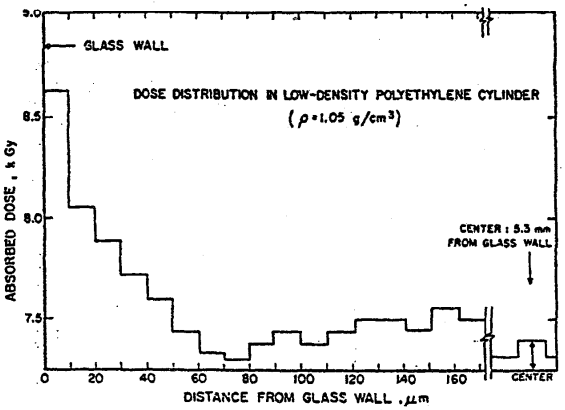

Fig. 19. Depth-dose distribution near the inner surface of 2-ml glass ampoule in a stack of thin polyvinyl pyrrolidone radiochromic dye films (thickness of each: 10 μm) backed by low-density polyethylene cylinders. At the center of the cylinder were three of the dye film dosimeters held in a central bisecting plane. The ampoule had 0.6 mm thick glass walls and was held tightly in a polystyrene cylinder with a 4.7 mm wall thickness. The $^{60}$Co gamma radiation field was coaxially symmetric around the ampoule [16].

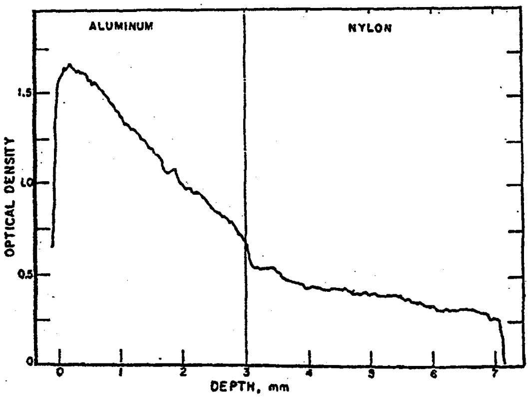

Fig. 20. Microdensitometer trace of optical density variation in a thin nylon radiochromic dosimeter film strip placed across interfaces between slabs of aluminum and nylon and irradiated from the left by $^{137}$Cs gamma rays.

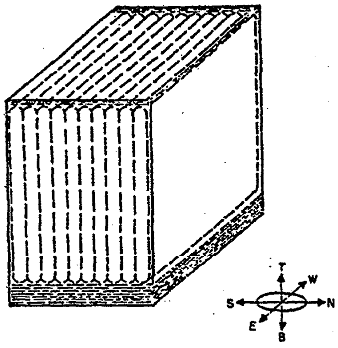

Fig. 21. Typical product box containing relatively homogeneous product arranged vertically in a box limit with cardboard sheets, for irradiation from S and N sides by a vertical $^{60}$Co gamma-ray source plaque [56].

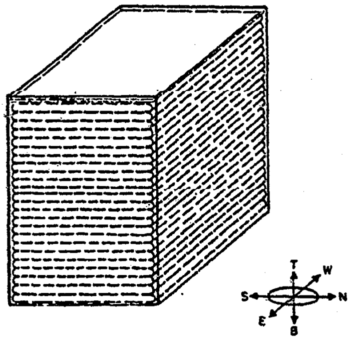

Fig. 22. Typical product box containing relatively homogeneous product arranged horizontally in a box lined with cardboard sheets, for irradiation from S and N sides by a vertical $^{60}$Co gamma-ray source plaque [56].

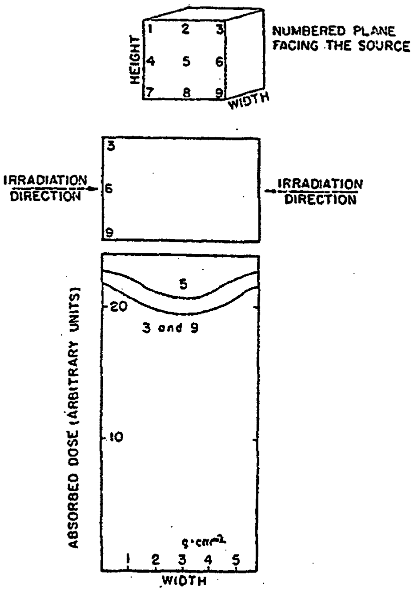

Fig. 23. Top: Numbered reference positions for dosimeter placement in irradiated box; middle: Indication of gamma-radiation direction for irradiation from both sides of the box; bottom: Lateral depth-dose distribution at the indicated dosimeter positions in the box [57].

somewhere along the central plane parallel to the plane of the source plaque, and the maximum dose lies somewhere near the plane surface closest to the source plaque (see Fig. 24) [8].

This idealized dose pattern may not be realized, however, if the product is considerably less homogeneous, or if there are large voids or air cavities within the product container (see Figs. 25 and 26). In this case it may be necessary to map the dose distribution field in more detail, either by the placement of individual thin dosimeters at various strategic locations on different surfaces and within a typical dummy sample of heterogeneous products (see Figs. 26 and 27) or by placement of an array of strips of thin dosimeter materials throughout a product box (see Fig. 28) [56].

It must be kept in mind, however, that the ultimate aims of dose distribution measurements for a given radiation process are to determine accurately the locations and values of minimum and maximum dose, and to provide experimental assurance that routine dosimeters are capable of agreeing with primary standard measurements of absorbed dose over all practical values of product dwell time in the irradiator (see Fig. 29) [57]. Non-linearity of response of the dyed plastic dosimeters has been accounted for in these results.

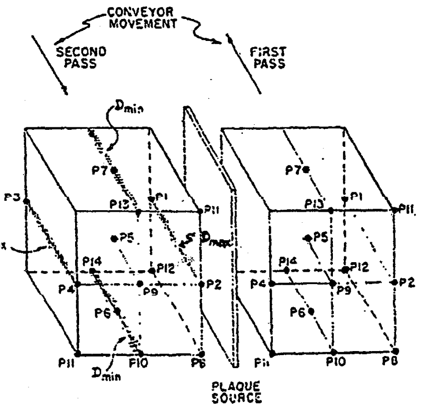

Fig. 24. Two single-direction passes of a rectangular package, once on each side of a stationary gamma-ray plaque source, with the regions of minimum and maximum dose after the second pass indicated by hatch marks [8].

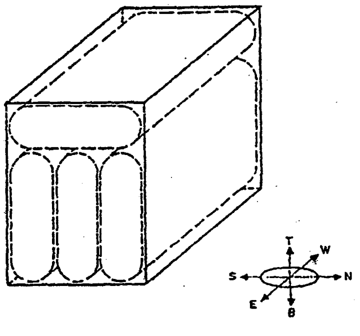

Fig. 25. Typical product box containing relatively large items to be sterilized, resulting in appreciable air cavities [56].

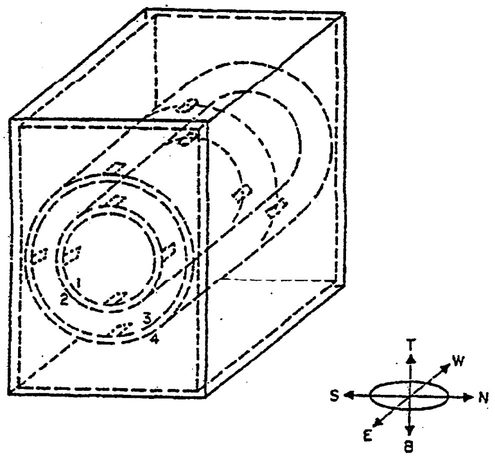

Fig. 26. A cardboard box containing concentric cylinders (length 42 cm) of polypropylene: inner cylinder: thickness 0.53 cm and outer diameter 11.2 cm; outer cylinder: thickness 0.68 cm and outer diameter 19.0 cm [16]. The box was irradiated by gamma rays from two sides, south and north, using a large $^{60}$Co source plaque. The cylinder surfaces are indicated by numbers 1, 2, 3, and 4. Dosimeter film locations are indicated both in a bisecting plane perpendicular to the cylinder axes and at the east end of the cylinders.

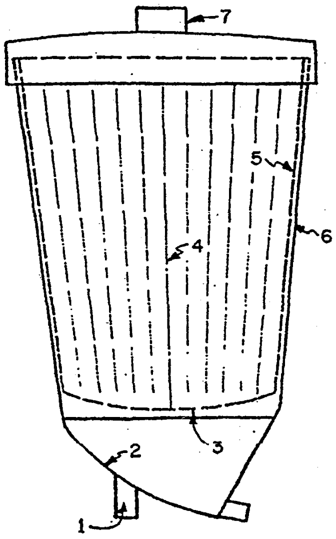

Fig. 27. Cross-section of a heterogeneous product irradiated symmetrically from the left and right by gamma-radiation from a $^{60}$Co source plaque. Position numbers indicate where calibrated radiochromic dye film dosimeters might be placed in order to determine extreme values of absorbed dose [15].

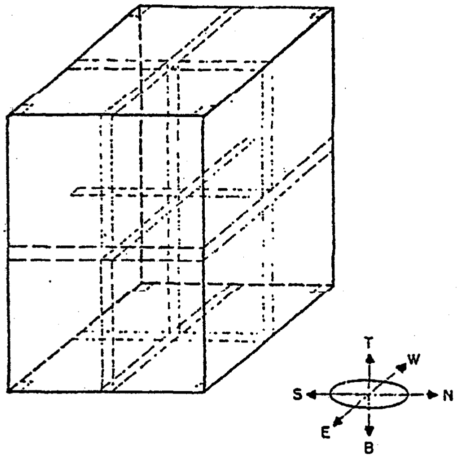

Fig. 28. A product box with positions of radiochromic dye film strips. Small pieces of dye film are placed in the eight corners of the box, which moves in an east-to-west direction in passage by the vertical $^{60}$Co gamma-ray source plaque and is then turned 180° and irradiated from the other side (north and south sides) [15].

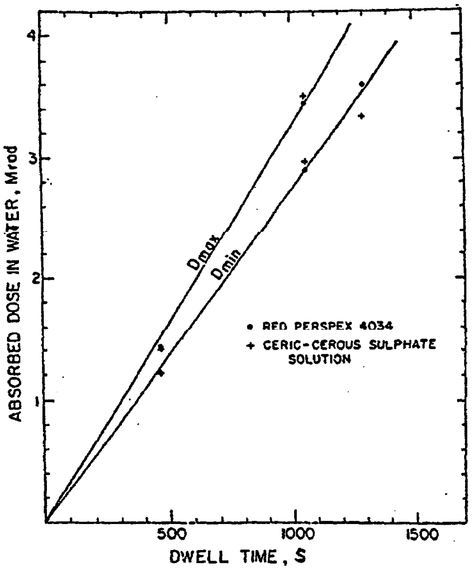

Fig. 29. Absorbed dose in water as measured by the indicated dosimeters in a dummy product versus dwell time in a shuffle-dwell gamma-ray irradiation [57].

## CONCLUSION

The main sources of uncertainty in routine dosimetry applied to radiation steril zation have been described. The most expedient ways to deal with these causes o error and imprecision in commissioning dosimetry and routine sterility control i production are:

1. Proper and up-to-date calibration and traceability to primary standards usin irradiation conditions as close as possible to those on the radiation processing line.

2. Either using calibrated dosimeters similar in radiation absorption properties to those of the irradiated substance of interest (i.e. biological matter, certain plastics, etc.) or knowing the approximate radiation spectra of interest at given locations in irradiated products, so that meaningful corrections can be applied for differences in absorption cross-sections.

3. Making suitable corrections for systematic errors in dose interpretations (instability, temperature and humidity dependence, non-linearities of response).

4. Use of correct and reproducible methods of read-out (e.g. spectrophotometry, optical densitometry, electropotentiometry, etc.).

5. Appropriate application of dosimeters according to their geometries and response characteristics.

## REFERENCES

[1] C.W. Bruch, Sterility assurance in medical supplies sterilized by gamma radiation. *Proceedings of Gamma Radiation Processing Seminar*, Atomic Energy of Canada, Ltd., Commercial Products, Ottawa, Canada 102 (1975).

[2] United States *Pharmacopeia XIX*, Mack Publishing Company, 20th and North Hampton Streets, Easton, PA 18042 (1975).

[3] W.L. McLaughlin, J.C. Humphreys, S.E. Chappell, T.A. Olejnik, and C.E. Fox, Physical measurements for quality control in industrial radiation sterilization, *Physics in Industry*, (E.O'Mongain and C.P. O'Toole, eds.) Proceedings of International Conference sponsored by IUPAP, Dublin, Ireland, Pergamon Press, Oxford 567 (1976).

[4] W.L. McLaughlin, Radiation measurements and quality control, Proceedings of 1st Intern. Meeting on Radiation Processing, Puerto Rico, 1976. (J. Silverman and A. van Dyken, eds.); *Radiat. Phys. Chem. 9*, 147-181 (1977).

[5] I.G. Draganić, Liquid chemical dosimeters, *Sterilization by Ionizing Radiation*, Vol. I (E.R.L. Gaughran and A.J. Goudie, eds.) Multiscience, Montreal 253-269 (1974).

[6] B.B. Radak and V.M. Marković, Calorimetry, Chap. 3 in *Manual on Radiation Dosimetry* (N.W. Holm and R.J. Berry, eds.) Marcel Dekker (1970).

[7] J.W. Boag, Ionization chambers, Chap. 9 in *Radiation Dosimetry*, Vol. II (F.H. Attix and W.C. Roesch, eds.) 2nd ed., Academic Press, New York (1966).

[8] K.H. Chadwick, D.A.E. Ehlermann, and W.L. McLaughlin, *Manual of Food Irradiation Dosimetry*, Technical Report Series No. 178, International Atomic Energy Agency, Vienna (1977).

[9] A. Miller, E. Bjergbakke, and W.L. McLaughlin, Some limitations in the use of plastic and dyed plastic dosimeters, *Int. J. Appl. Radiat. Isotopes 16*, 611-620 (1975).

[10] W.L. McLaughlin, P.E. Hjortenberg, and B.B. Radak, Absorbed dose measurements with thin films, *Dosimetry in Agriculture, Industry, Biology, and Medicine*, (Proc. Sympos., Vienna, 1972) International Atomic Energy Agency, Vienna 577-597 (1973).

[11] W.L. McLaughlin, Solid-phase chemical dosimeters, *Sterilization by Ionizing Radiation*, Vol. I (E.R.L. Gaughran and A.J. Goudie, eds.) Multiscience, Montreal 219-252 (1974).

[12] W.L. McLaughlin, R.D. Jarrett, and T.A. Olejnik, Dosimetry, Chap. 7 in *Preservation of Food by Ionizing Radiation*, Vol. I (E.S. Josephson and M.S. Peterson, eds.) CRC Press, Cleveland (1979) (in press).

[13] W.R. Bruce and H.E. Johns, The spectra of x rays scattered in low atomic number materials, *Br. J. Radiol.*, *Suppl. No. 9* (1960).

[14] B. Petree and P. Lamperti, A comparison of absorbed dose determination in graphite by cavity ionization measurements and by calorimetry, *NBS J. Res. 71C*, 19 (1967).

[15] W.L. McLaughlin, Dosimetry standards for industrial radiation processing, *National and International Standardization of Radiation Dosimetry, Vol. I.* (Proc. Sympos. Atlanta, 1977) International Atomic Energy Agency, Vienna 89-106 (1978).

[16] W.L. McLaughlin, A national standardization programme for high-dose measurement, *International Standardization of High-Dose Radiation Measurement* (Proc. Advisory Group Meeting, Vienna, 1978) International Atomic Energy Agency,

[17] M.B. Anderson and D.L. Smyth, Gammacell 220 spectra, Atomic Energy of Canada Ltd., July 1967 (unpublished data).

[18] T.E. Burlin, Cavity-chamber theory, Chap. 8 in Radiation Dosimetry, Vol. I, (F.H. Attix and W.C. Roesch, eds.) 2nd ed., Academic Press, New York (1968).

[19] F.K. Chan and T.E. Burlin, An experimental examination of a general cavity theory using a solid state dosimeter. Br. J. Radiol. 43, 54 (1970)

[20] M.J. Berger and S.M. Seltzer, Tables of energy losses and ranges of electrons and positrons, in NASA SP-3012 and NASA SP-3036, National Technical Informati Service, Springfield, VA (1964, 1966).

[21] L. Pages, E. Bertel, H. Joffre, and L. Sklavenitis, Energy loss, range, and bremsstrahlung yields for 10 keV to 100 MeV electrons in various elements and chemical compounds, Atomic Data 4, 1 (1972)

[22] J.H. Hubbell, Photon mass attenuation and mass energy absorption coefficients for H, C, N. O, Ar, and seven mixtures from 0.1 keV to 20 MeV, Radiat. Res. 70, 58 (1977).

[23] D.R. White, Tissue substitutes in experimental radiation physics, Med. Phys 5, 467 (1978).

[24] H. Fricke and E.J. Hart, Chemical dosimetry, Chap. 12 in Radiation Dosimetry, Vol. II, (F.H. Attix and W.C. Roesch, eds.) 2nd Ed., Academic Press, New York (1966).

[25] American Society of Testing and Materials, Absorbed gamma radiation dose in the Fricke dosimeter, American Standard Method of Test D1671-63, ASTM Standards, Part 27, ASTM Philadelphia 529 (1965).

[26] S.I. Taimuty, L.H. Towle, and D.L. Peterson, Ceric dosimetry routine use at $10^5$ - $10^7$ rads, Nucleonics 17 (8) 103 (1959).

[27] American Society of Testing and Materials, Absorbed gamma and electron radiation dose with the ceric sulfate dosimeter, Standard Method of Test D3001-71 1971 Book of ASTM Standards, Part 27, ASTM, Philadelphia, PA, 1, (1971).

[28] D. Ražem and I. Dvornik, Application of the ethanol-chlorobenzene dosimeter to electron-beam and gamma radiation dosimetry-III, Tissue equivalent dosimetry, Radiation Preservation of Food (Proc. Sympos., Bombay, 1972) International Atomic Energy Agency, Vienna 537 (1973).

[29] D. Ražem and I. Dvornik, The applications of the ethanol-chlorobenzene dosimeter to electron beam and gamma radiation dosimetry-II $^{60}$Co gamma rays, Dosimetry in Agriculture, Industry, Biology, and Medicine (Proc. Sympos. Vienna, 1972) International Atomic Energy Agency, Vienna (1973).

[30] G. Földiak, Zs. Horvath, and V. Stenger, Routine dosimetry for high-activity gamma-radiation facilities, Dosimetry in Agriculture, Industry, Biology, and Medicine (Proc. Sympos., Vienna, 1972) International Atomic Energy Agency, Vienna (1973) 367.

[31] R.W. Mathews, Potentiometric estimation of megarad dose with ceric-cerous system, Int. J. Appl. Radiat. Isotopes 23, 179 (1972).

[32] W.L. McLaughlin and M. Kosanić, The gamma-ray response of pararosaniline cyanide dosimeter solutions, Int. J. Appl. Radiat. Isotopes 25, 249 (1974)

[33] M.M. Kosanić, M.T. Nenadović, B.B. Radak, V.M. Marković, and W.L. McLaughlin, Liquid radiochromic dye dosimetry for continuous and pulsed radiation fields over a wide range of energy flux densities, Int. J. Appl. Radiat. Isotopes 28, 313 (1977).

[34] K.H. Chadwick, D. Rintjema, and W.R.R. ten Broeke, The accuracy of the calibration curve of the clear Perspex dose meter, Food Preservation by Irradiation (Proc. Sympos., Wageningen, 1977) International Atomic Energy Agency, Vienna (1978).

[35] J.R. Puig, J. Laizier, and F. Sundardi, Le Film TAC dosimetre plastique pour la mesure pratique des doses d'irradiation recues en sterilisation, Radiosterilization of Medical Products (Proc. Sympos., Bombay, 1974) International Atomic Energy Agency, Vienna (1975).

[36] A. Charlesby, Comparison of alpha-, gamma-, and ultra-violet effects in irradiated polyethylene unsaturation changes, Radiation Chemistry (Proc. Sympos., Tihany, 1962) Akademiai Kiado; Budapest (1962) pp. 175-183.

[37] Th. Grünewald and G. Rumpf, Ein einfaches Polyäthylen-Dosimeter Atompraxis 11 (2), 95-98 (1965).

[38] B. Whittaker, Recent developments in poly (methyl methacrylate) dye systems for dosimetry purposes, Radiation Dose and Dose Rate Measurements in the Megarad Range (Proc. Sympos., Teddington, 1970) U.K. Panel on Gamma and Electron Irradiation, National Physical Laboratory, Teddington (1970) 11.

[39] W.L. McLaughlin, A. Miller, S. Fidán, K. Pejtersen, and W. Batsberg Pedersen, Radiochromic plastic films for accurate measurement of radiation absorbed doses and dose distributions, Radiat. Phys. Chem. 10, 119 (1977).

[40] A.D. Kantz and K.C. Humphreys, Radiochromics: A radiation monitoring systems, Radiation Processing (Trans. 1st Intern. Meeting, Puerto Riso, 1976) (J. Silverman and A. Van Dyken, eds); Rad. Phys. Chem. 9, 737 (1977).

[41] A. Charlesby and A.J. Woods, Radiation dosimetry with dyed cellophane, Int. J. Appl. Radiat. Isotopes 14, 413 (1963).

[42] N. Goldstein, Cinemoid color films, Manual on Radiation Dosimetry, (N.W. Holm and R.J. Berry, eds.) Marcel Dekker, New York (1970) 371.

[43] F. Bermann, H. de Choudens, and S. Descours, Application a la dosimetrie de la mésure par resonance paramagnetique electronique des radicaux libres creés dans les acides amines, Advances of Physical and Biological Radiation Detectors (Proc. Symp., Vienna, 1971) International Atomic Energy Agency, Vienna (1971) 311.

[44] D.F. Regulla and U. Deffner, Dosimetry in the megarad range by means of ESR-spectrometry of free radicals of amino acids, Radiation for Pollution Abatement (Proc. Conf., Munich, 1976) European Soc. Nucl. Methods in Agriculture, Munich (1976) 21.

[45] D.I. Thwaites, G. Buchan, K.V. Ettinger, J.R. Mallard, and A. Takavan, A new sensitive technique for study of radiation effects in amino acids, Int. J. Appl. Radiat. Isotopes 27, 663 (1976).

[46] K.V. Ettinger, A. Takavar, and J.R. Mallard, Development of lyoluminescence dosimetry system for radiation processing of food, Food Preservation by Irradiation (Proc. Sympos., Wageningen, 1977) International Atomic Energy Agency, Vienna (1978).

[47] K.J. Puite, D. Rintjima, and D. J. M. Crebolder, High dose level dosimetry using the lyoluminescence technique, Food Preservation by Irradiation (Proc. Sympos., Wageningen, 1977) International Atomic Energy Agency, Vienna (1978).

[48] R.W. Mathews, The ceric-cerous dosimeter and degraded energy spectra in industrial gamma irradiators, Int. J. Appl. Radiat. Isotopes 37, 188 (1976)

[49] A. Brynjolfsson, A significant correction factor in gamma ray dosimetry, Chap. 8 in Radiation Chemistry, Vol. I (E.J. Hart, ed.) America Chemical Society, Washington, D.C. (1968).

[50] W.L. McLaughlin, J.C. Humphreys, B.B. Radak, A. Miller, and T.A. Olejnik, The response of plastic dosimeters to gamma rays and electrons at high absorbed dose rates, Trans. 2nd Int. Meeting on Radiation Processing, Miami, 1978 (J. Silverman, ed.); Radiat. Phys. Chem.(1979) (in press).

[51] T.A. Olejnik, Effects of the physical environment within large gamma-ray irradiations on red Perspex dosimeter response, Int. J. Appl. Radiat. Isotope (in press).

[52] H. Levine, W.L. McLaughlin, and A. Miller, Temperature and humidity effects on the gamma-ray response and stability of plastic and dyed plastic dosimeters, Trans. 2nd Int. Meeting on Radiation Processing, Miami, 1978 (J. Silverman, ed.); Radiat. Phys. Chem, (1979) (in press).

[53] T.A. Olejnik, Red 4034 Perspex dosimeters in industrial radiation sterilization process control, Trans. 2nd Int. Meeting on Radiation Processing, Miami, 1978 (J. Silverman, ed.); Radiat. Phys. Chem. (1979) (in press).

[54] M. Ehrlich, Influence of size of $CaF_2$:Mn thermoluminescence dosimeters in $^{60}$Co gamma-ray dosimetry in extended media, Luminescence Dosimetry, Proc. Commission, Roskilde, Denmark (1971) p. 550.

[55] T.P. Loftus and J.T. Weaver, Standardization of $^{60}$Co and $^{137}$Cs gamma-ray beams in terms of exposure, NBS J. Res. 78A, 465-476 (1974).

[56] W.L. McLaughlin, J.C. Humphreys, S.E. Chappell, and T.A. Olejnik, "Dose distributions in various products irradiated by large $^{60}$Co gamma-ray plaques", NBS Report (to be published).

[57] B.B. Radak, V.M. Marković, and W.L. McLaughlin, Dosimetry for the commissioning of a versatile irradiation plant, Trans. 2nd Int. Meeting on Radiation Processing, Miami, 1978 (J. Silverman, ed.); Rad. Phys. Chem. (1979) (in press).

as crosslinking agents, and radiation which can promote crosslinking in many polymers can of course also induce cancer. In fact for some time the possibility was considered that crosslinking between DNA strands might be involved in cancer. Radiation protectors effective in biological systems are often effective in inhibiting crosslinking for example.

There seems to be considerable scope in extending this type of investigation, to determine how far the biological changes are related to those induced in these far simpler materials, where the physical and chemical processes can be more readily followed.

/KJ